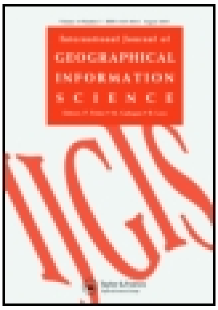

International Journal of Geographical Information Science
Publication details, including instructions for authors and subscription information:
http://www.tandfonline.com/loi/tgis20

An improved artificial immune system for seeking the Pareto front of land-use allocation problem in large areas

Kangning Huang [a] , Xiaoping Liu [a] , Xia Li [a] , Jiayong Liang [a] & Shenjing He [a]

[a] School of Geography and Planning, and Guangdong Key Laboratory for Urbanization and Geo-simulation, Sun Yat-sen University, Guangzhou, Guangdong, PR China

Version of record first published: 08 Nov 2012.

International Journal of Geographical Information Science
i*First*, 2012, 1–25

An improved artificial immune system for seeking the Pareto front of land-use allocation problem in large areas

Kangning Huang, Xiaoping Liu*, Xia Li, Jiayong Liang and Shenjing He

School of Geography and Planning, and Guangdong Key Laboratory for Urbanization and Geo-simulation, Sun Yat-sen University, Guangzhou, Guangdong, PR China

(*Received 16 November 2011; final version received 11 September 2012*)

The Pareto front can provide valuable information on land-use planning decision by revealing the possible trade-offs among multiple, conflicting objectives. However, seeking the Pareto front of land-use allocation is much more difficult than finding a unique optimal solution, especially when dealing with large-area regions. This article proposes an improved artificial immune system for multi-objective land-use allocation (AIS-MOLA) to tackle this challenging task. The proposed AIS is equipped with three modified operators, namely (1) a heuristic hypermutation based on compromise programming, (2) a non-dominated neighbour-based proportional cloning and (3) a novel crossover operator that preserves connected patches. To validate the proposed algorithm, it was applied in a hypothetical land-use allocation problem. Compared with the Pareto Simulated Annealing (PSA) method, AIS-MOLA can generate solutions more approximate to the Pareto front, with computation time amounting to only 5.1% of PSA. In addition, AIS-MOLA was also applied in the case study of Panyu, Guangdong, PR China, a large area with 389 × 337 cells. Experimental results indicate that this algorithm, even dealing with large-area land-use allocation problems, is capable of generating optimal alternative solutions approximate to the true Pareto front. Moreover, the distribution of these solutions can quantitatively demonstrate the complex trade-offs between the spatial suitability and the compactness in the study area. Software and supplementary materials are available at http://www.geosimulation.cn/AIS-MOLA/.

Keywords: land-use allocation problem; multi-objective optimization; Pareto front; artificial immune system

1. Introduction

The land-use allocation problem has been encountered in many fields of applications, such as land-use planning, urban planning, habitat design, watershed management, forestry and local authority planning (Brookes 2001). All of these applications require the planner to find the optimal spatial allocation of different types of land-use units, which can be represented by either raster grid or polygons in geographic information system (GIS). This process of land-use allocation is essentially a combinatorial optimization problem (COP), with enormous amount of candidate combinations in the solution space. For instance, if there are K different land uses that need to be allocated in a raster-represented region, with a size of $R \times C$, then there exist $K^{R\times C}$ possible combinations. The enormous solution

*Corresponding author. Email: liuxp3@mail.sysu.edu.cn

ISSN 1365-8816 print/ISSN 1362-3087 online

http://dx.doi.org/10.1080/13658816.2012.730147
http://www.tandfonline.com

space makes it an NP-hard (non-deterministic polynomial-time hard) problem (Eldrandaly 2010).

In addition to the aforementioned enormous solution space issue, land-use allocation also needs to simultaneously optimize several different objectives, such as those that consider site attributes (e.g. suitability, cost and environmental impacts) or aggregation attributes (e.g. shape, contiguity and compactness) (Cova and Church 2000). Considering that these multiple objectives usually conflict with each other, there hardly exists a unique solution that optimizes all of them but a set of solutions known as Pareto-optimal alternatives (Pareto 1971), whose image in objective space is called the Pareto front. According to previous studies (Hopkins *et al*. 1982, Brill Jr *et al.* 1990, Keeney and Raiffa 1993), the evenly distributed Pareto optimal alternatives can remarkably represent the possible trade-offs between conflicting objectives. These trade-offs inform the land-use planners about how much deterioration on other objectives will be caused by improving one certain objective and will surely improve the reliability of the land-use planning decision. Therefore, seeking the Pareto optimal alternatives should be taken into account when dealing with land-use allocation problems. However, this task is much more challenging than finding a unique optimal solution. This is because the computational complexity is increased by generating multiple solutions and also because of the difficulty associated with maintaining a desirable distribution of the alternative solutions.

To overcome those difficulties and seek well-distributed alternatives, various techniques have been developed. Earlier attempts (Hopkins *et al*. 1982, Brill Jr *et al.* 1990, Keeney and Raiffa 1993) turned the multi-objective optimization problem (MOP) into a single-objective optimization problem (SOP) by taking the linear weighted sum of the multiple objectives. This approach can somehow learn the shape of the Pareto front by iteratively adjusting the associated weights of different objectives and repeatedly applying the single-objective optimization techniques. In previous studies, the single-objective optimization techniques for land-use allocation problems were divided into deterministic and heuristic ones. Deterministic techniques can achieve the optimal land allocation (Koski 1988, Jahn *et al*. 1991), whereas their application is limited by the requirement of a well-formulated objective function and a small number of allocable land units (Campbell *et al.* 1992, Crohn and Thomas 1998, Aerts *et al.* 2003). On the other hand, heuristic techniques, although cannot guarantee the optimal land-use combination, are able to generate a near-optimal one within a reasonable time by simulating physical phenomena (Aerts and Heuvelink 2002, Santé-Riveira *et al.* 2008), biological processes (Brookes 2001) and swarm behaviour (Chen *et al.* 2010). Nevertheless, no matter what optimization techniques are used, the linear weighting approach suffers from two serious drawbacks (Das and Dennis 1997), namely (1) the generated solutions may be unevenly distributed and (2) the concave part of the Pareto front may be disregarded. Huang *et al.* (2008) successfully overcame these two drawbacks in conventional MOPs by proposing a strategy that tunes the searching direction of each SOP according to the largest unexplored regions. In spite of that, since there is still the need to solve SOPs repeatedly, it is inefficient to apply Huang's searching strategy in an NP-hard problem like land-use allocation.

Recently, other researches tried to extend the single-objective heuristic algorithms, so that they can optimize multiple objectives simultaneously. Various multi-objective heuristic algorithms have been proposed, for example, Pareto Simulated Annealing (PSA) (Czyzak and Jaszkiewicz 1998), Non-Dominated Sorting Genetic Algorithm (NSGA) (Srinivas and Deb 1994), Pareto Archive Evolutionary Strategy (PAES) (Knowles and Corne 2000), Multi-Objective Particle Swarm Optimization (MOPSO) (Coello *et al*. 2004) and Multi-Objective Immune System Algorithm (MISA) (Coello and Cortés 2005). These algorithms allow the solving of MOPs with complicated factors, including huge solution space, non-linearity and non-standard underlying objective function (Jones *et al*. 2002), which make them potentially suitable for land-use allocation problems. However, despite these extraordinary characteristics, there are still rare attempts to use them for solving MOLA problems. Among these attempts, evolutionary algorithms (EAs) are the most popular optimization techniques. Matthews *et al.* (2001) first applied the Multi-Objective Genetic Algorithm (mGA) in land-use planning, using the land-block and percentage and priority (P&P) representations. Then, Bennett *et al.* (2004) developed an EA and Integer Programming Hybrid Algorithm to explore geographic consequences of public policies. Later, Roberts *et al*. (2011) used Non-Dominated Sorting Genetic Algorithm-II (NSGA-II) and graph coding to estimate the Pareto optimal set of landscape designs. For the sake of easy encoding and manipulating, all of these evolutionary approaches use the polygon-based presentation, whereas this representation precludes them from modifying the shapes of land-use patterns because the shapes of polygon-represented land-use blocks are predefined. Moreover, since each polygon varies in area, different polygon-represented land-use combinations vary in land-use area proportion. This issue makes them impractical in some countries or regions like China, where land-use area proportions are predefined and strictly supervised by the authorities.

Grid representation, rather than polygon, is efficient and effective to modify the shapes of land-use patterns, and it has been implemented in recent researches. Cao *et al.* (2011) proposed a grid-represented spatial optimization model based on NSGA-II-Multi-objective Optimization of Land Use (MOLU), but the mutation and crossover operator designed in this model lacked the capability to maintain constant land-use area proportions. Besides, Duh and Brown (2007) studied the spatial pattern allocation problems with grid representation and successfully generated a satisfactory set of Pareto optimal alternatives using PSA. Although PSA may be more computationally expensive than the EAs (Youssef *et al*. 2001), it is able to obtain comparable solutions for MOPs (Nam and Park 2000). However, that approach proposed by Duh and Brown (2007) was only applied to a simplified hypothetical problem with an 18×18 gridded space and two allocable land-use types, which may be inconsistent with reality. Consequently, there are still demands for multi-objective techniques that are capable of fulfilling the needs of real-world allocation problems, with large-area and multi-type land use.

In this article, we focus on the grid-represented MOLA problem with area constraints and strive to resolve such issue in large-area regions by using a modified version of the artificial immune system (AIS). Algorithms based on AIS are inspired by the highly evolved, parallel and distributed adaptive human immune system (HIS). This category of algorithms follows the evolution procedure from evolutionary computation, combined with the clonal selection and affinity maturation strategies imitating the immunological process. Besides the implementations in many other fields (Dasgupta and Nino 2008), AIS have also been successfully applied in some complex geographical problems, for example, simulating land-use dynamics (Liu *et al*. 2010) and zoning farmland protection (Liu *et al*. 2011). These studies have shown that AIS is potentially useful in handling complex spatial problems. Moreover, according to previous researches (Coello and Cortés 2005, Jiao *et al.* 2005, Gong 2008), multi-objective AIS algorithms, the extensions of AIS, outperform many other MOP approaches in solving high-dimensional problems. Therefore, we considered that AIS has the potential to cope with the MOLA problem.

However, since land-use allocation is non-standard formulated and with enormous complexity, modifications must be made, before applying AIS to seek the Pareto front of the grid-represented land-use allocation problems. In this article, three modified operators have been designed, namely (1) a heuristic hypermutation based on compromise programming (CP) is developed to improve efficiency, (2) the non-dominated neighbour-based selection and proportional cloning method is introduced to make the immune system pay more attention to less explored regions and (3) a novel crossover operator that preserves connected land-use patches is designed to generate better solutions. The effectiveness and efficiency of the proposed approach are validated by applying it in a hypothetical land-use allocation problem. Meanwhile, its performance on this problem is compared with that of the PSA approach. Last but not least, an implementation of our approach on Panyu, a region in Guangzhou, PR China, demonstrates its capability in revealing possible trade-offs in real-world land-use allocation problem.

The remainder of this article is organized as follows. The mathematical formulation of land-use allocation problem and the definition of Pareto optimal alternatives and Pareto front are explained in Section 2. The main procedure and the three modified operators of AIS-MOLA are presented in Section 3. Then, the experiments based on a hypothetical data set and a real-world data set are then conducted and discussed in Section 4. Finally, in Section 5, conclusions are drawn based on previous experiments.

2. Multi-objective land-use allocation problem

2.1. Model of land-use allocation problem

The land-use allocation problem M can be defined as (Aerts and Heuvelink 2002):

$$M = (S, \Omega, f) \tag{1}$$

where S denotes the set of all candidate solutions, Ω is a set of constraints and f is an objective function. When simultaneously optimizing multiple objectives, the definition above can be extended as

$$\begin{cases} M = (S, \Omega, \mathbf{F}) \\ \mathbf{F} = [f_1, f_2, \cdots, f_k]^{\mathrm{T}} \end{cases} \tag{2}$$

F is a k-dimensional vector, containing all objective functions. Here, the study region is represented as a two-dimensional grid with R rows and C columns, and there are K different kinds of land uses that can be allocated to each cell (i,j). The spatial pattern of the allocation solution can be formulated mathematically as a binary decision variable x_{ijk}, with 1 if the kth land use is allocated to cell (i,j) and 0 otherwise. In such way, the solution is represented as an $R \times C \times K$ dimension binary decision vector $\mathbf{X} = \{x_{ijk}\}$. Suppose the pre-specified amount of cells for the kth land use is Q_k and only one land use can be allocated to each cell, then the decision vector **X** must satisfy the following constraints:

$$\begin{cases} \sum_{k=1}^{K} x_{ijk} = 1, \forall ij \\ \sum_{i=1}^{R} \sum_{j=1}^{C} x_{ijk} = Q_k, \forall k \end{cases} \tag{3}$$

As mentioned in Section 1, multiple conflicting objectives may be involved in land-use allocation problems. All in all, these objectives can be classified into two categories, namely (1) those that consider site attributes and (2) those that take aggregation attributes into account. For simplicity and better visualization of the Pareto front, only two objectives of land allocation (Siitonen *et al*. 2003) are included in this study, namely (1) maximizing land-use suitability and (2) maximizing spatial compactness, which are explained as follows:

(1) Maximizing the suitability of land use
Set suit_{ijk} as the suitability of cell (i, j) for the kth land use, and the total suitability of the study region is

$$\mathrm{suit}_{\mathrm{total}} = \sum_{i=1}^{R}\sum_{j=1}^{C}\sum_{k=1}^{K}\left(\mathrm{suit}_{ijk} \cdot x_{ijk}\right) \tag{4}$$

To define a dimensionless objective, we normalize the suitability by

$$f_{\mathrm{suit}} = \frac{\mathrm{suit}_{\mathrm{total}} - \mathrm{suit}_{\mathrm{min}}}{\mathrm{suit}_{\mathrm{max}} - \mathrm{suit}_{\mathrm{min}}} \tag{5}$$

where $\mathrm{suit}_{\mathrm{max}}$ is the total suitability when each cell is allocated by a land use with maximum suitability, and $\mathrm{suit}_{\mathrm{min}}$ is that allocated by those with minimum suitability. The value of f_{suit} is within the range of [0,1]

(2) Maximizing the spatial compactness of land use
Set L_{total} as the total perimeter of all land-use patches. The shorter the total perimeter, the more compact is the allocation solution. The compactness objective is defined as follows:

$$f_{\mathrm{comp}} = \frac{L_{\mathrm{total}} - L_{\mathrm{min}}}{L_{\mathrm{max}} - L_{\mathrm{min}}} \tag{6}$$

where L_{max} and L_{min} can be calculated as

$$L_{\mathrm{max}} = \sum_{k=1}^{K}(4Q_k) \tag{7}$$

$$L_{\mathrm{min}} = \sum_{k=1}^{K}\left(2\pi\sqrt{\frac{Q_k}{\pi}}\right) \tag{8}$$

If every selected site is separated from each other, the possible maximum perimeter L_{max} can be obtained by Equation (7). As the amount of each land use Q_k is known, the possible minimum perimeter can be formulated as the perimeter of a circle with the same area by Equation (8).

2.2. Definition of Pareto optimal

Multi-objective optimization (Deb 2001) seeks to optimize a vector of functions $\mathbf{F}(\mathbf{x})$ with respect to vector $\mathbf{x} = [x_1, x_2, \cdots, x_n]^{\mathrm{T}} \in \Omega$, which satisfies the condition described in Equation (9). Minimization problems can be transformed into maximization problems by taking the reciprocal or negative of the objectives.

$$\begin{cases} \max \mathbf{F}(\mathbf{x}) = [f_1(\mathbf{x}), f_2(\mathbf{x}), \cdots, f_k(\mathbf{x})]^{\mathrm{T}} \in \Re^k \\ \text{subject to } \mathbf{x} = [x_1, x_2, \cdots, x_n]^{\mathrm{T}} \in \Omega \end{cases} \tag{9}$$

Vector $\mathbf{F}(\mathbf{x})$ is called the objective vector defined in the objective space. Similarly, vector $\mathbf{x}$ is called the decision vector defined in the decision space, and Ω is the feasible region, a subset of the decision space. When optimizing a vector rather than a single number, a solution is really improved only if the improvement of one objective does not worsen others. Following this principle, a decision vector $\mathbf{x}_A \in \Omega$ is said to *dominate* another vector $\mathbf{x}_B \in \Omega$ (written as $\mathbf{x}_A \succ \mathbf{x}_B$) if Equation (10) is satisfied.

$$\forall i = 1, 2, \ldots, k \ \text{ s.t. } f_i(\mathbf{x}_A) \geq f_i(\mathbf{x}_B) \wedge \exists j = 1, 2, \ldots, k \ \text{ subject to } \ f_i(\mathbf{x}_A) > f_i(\mathbf{x}_B) \tag{10}$$

For a solution $\mathbf{x}^* \in \Omega$, if another $\mathbf{x} \in \Omega$ does not exist, such that $\mathbf{x} \succ \mathbf{x}^*$, it is said to be a *Pareto optimal solution* or *a non-dominated solution*. In other words, a Pareto optimal solution is a solution that cannot be improved further.

More importantly, the *Pareto optimal set* is defined in Equation (11), and the corresponding image under the objective space is defined in Equation (12), which is called the *Pareto optimal front*.

$$\mathbf{P}^* = \left\{ \mathbf{x}^* \in \Omega | \neg \exists \mathbf{x} \in \Omega, \mathbf{x} \succ \mathbf{x}^* \right\} \tag{11}$$

$$\mathbf{PF}^* = \left\{ \mathbf{F}\left(\mathbf{x}^*\right) | \mathbf{x}^* \in \mathbf{P}^* \right\} \tag{12}$$

An evenly distributed Pareto optimal set is the ultimate goal of MOPs; therefore, such set of land-use allocation problem is also the goal of the proposed algorithm.

3. Artificial immune system for multi-objective land allocation

The AIS is capable of solving various problems by simulating the behaviour of immunological processes. These processes that protect us on a daily basis are powered by clonal selection and affinity maturation by hypermutation (Garrett 2005). To adapt to new types of antigens, the antibody population within the system evolves by the processes of recombination, hypermutation and clonal selection. In AIS, the encoded solutions of the problem are treated as artificial antibodies, and the immunological processes will be implemented on them. The recombination and hypermutation are similar to the crossover and mutation operations in genetic algorithm (GA), which makes the antibodies to evolve and adapt to the problem. The clonal selection, on the other hand, is the major difference of AIS from GA. In clonal selection process, the cloning proportion of each antibody is based on its affinities, including (1) affinity between antibody and antigens and (2) affinity between itself and other antibodies. The former affinity preserves the well-performed antibodies, whereas the latter one maintains the diversity of the antibody population. These characteristics make AIS more efficient in exploring the solution space and maintaining the even distribution of found alternatives.

We modify and extend AIS to efficiently solve a MOLA problem with large area. The artificial antibody in AIS is encoded as the same binary vector $\mathbf{X} = \left\{x_{ijk}\right\}$ used to formulate the problem. Then, three basic operators of AIS (recombination, hypermutation and clonal

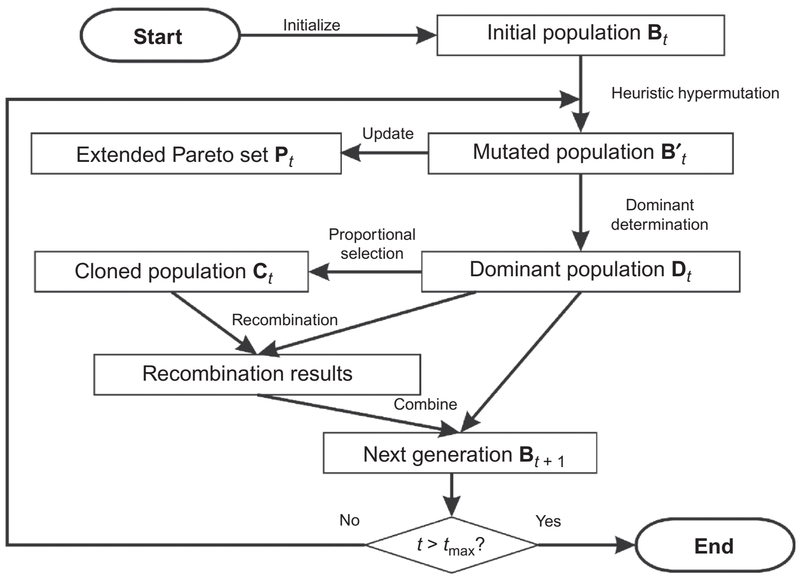

Figure 1. The main procedure of AIS-MOLA.

selection) are modified to better approximate the Pareto optimal alternatives of the land-use allocation problem. The main procedure of AIS-MOLA is as follows (also illustrated in Figure 1):

Step 1: *Initialization*. Initialize the antibody population $\mathbf{B}_t$ as a set of randomly generated decision vectors with size n_B. Create the initial extended Pareto set as $\mathbf{P}_t = \phi$. Set $t = 0$.

Step 2: *Hypermutation*. Apply hypermutation operator $\mathbf{T}^H(*)$ to $\mathbf{B}_t$ and get the resulting population $\mathbf{B}_t^*$.

Step 3: *Update extended Pareto set*. Set the dominant population $\mathbf{D}_t$ as the dominant antibodies in $\mathbf{B}_t^*$. Copy $\mathbf{D}_t$ to the extended Pareto set and remove all dominated antibodies in $\mathbf{P}_t$.

Step 4: *Clonal selection*. Calculate the crowding distance of each antibody in $\mathbf{D}_t$ and then get the clonal population $\mathbf{C}_t$ by performing proportional cloning $\mathbf{T}^C(*)$ on $\mathbf{D}_t$.

Step 5: *Recombination*. Perform recombination $\mathbf{T}^R(*)$ on $\mathbf{C}_t$ with randomly selected antibodies from $\mathbf{D}_t$ and then get the next generation of antibody population $\mathbf{B}_{t+1}$ by combining the resulting population and $\mathbf{D}_t$.

Step 6: *Termination*. Set $t = t + 1$. If $t < t_{\max}$, go to step 2; otherwise, terminate the procedure.

The maximum iteration $t_{\max}$ will be reached when the algorithm converges to an optimal set of Pareto alternatives. If there are very few or no new dominant antibodies generated in the latest iteration, we can conclude that the algorithm has converged and should be terminated. During the iteration, the extended Pareto set $\mathbf{P}_t$ collects the antibody population at each generation and updates itself by removing all antibodies that are dominated. This extended set is used to preserve all possible Pareto optimal solutions during the optimization process. When the algorithm has been terminated, $\mathbf{P}_t$ will be the final output of the algorithm.

Among these steps, the modified operators for hypermutation (in step 2), clonal selection (in step 4) and recombination (in step 5) play key roles in the evolution of the antibody population. These operations will be described in detail as follows.

3.1. Heuristic hypermutation based on compromise programming

The heuristic hypermutation operator $\mathbf{T}^H(*)$ on the antibody population $\mathbf{B} = \{\mathbf{X}_1, \mathbf{X}_2, \ldots, \mathbf{X}_{|\mathbf{B}|}\}$ is defined as

$$\begin{aligned}\mathbf{T}^H(\mathbf{B}) &= \left\{\mathbf{T}^H(\mathbf{X}_1), \mathbf{T}^H(\mathbf{X}_2), \ldots, \mathbf{T}^H\left(\mathbf{X}_{|\mathbf{B}|}\right)\right\} \\ &= \left\{\text{mutate}(\mathbf{X}_1), \text{mutate}(\mathbf{X}_2), \ldots, \text{mutate}\left(\mathbf{X}_{|\mathbf{B}|}\right)\right\}\end{aligned} \tag{13}$$

The mutation is performed on each antibody in the population, trying to improve their performance. This operator adapts the hop–skip–jump (HSJ) technique (Brill *et al*. 1982) to alter the antibody. HSJ randomly selects two cells (e.g. (i_1,j_1) and (i_2,j_2)) with different land-use types, and then swaps these cells and revaluates the objective function. By HSJ we can obtain a modified solution from the previous one. This technique has been used as a local search strategy to achieve improved solutions in several other land-use allocation solutions (Brookes 2001, Ligmann-Zielinska *et al*. 2008, Santé-Riveira *et al.* 2008). However, because of the tremendous amount of candidates in a large-area land-use allocation problem, many times of HSJ must be implemented before achieving substantial improvement. Simply applying dominance (as discussed in Section 2.2) as accepting criteria in HSJ may be inefficient due to the relatively heavy computation of the determination of dominance. To improve the efficiency, we developed a mutation operator that combines HSJ techniques with CP.

CP, firstly proposed by Zeleny (1973), enables one to find a Pareto optimum by maximizing (or minimizing) a scalarized utility function. Unlike the regular linear weighted sum methods, CP is able to achieve those solutions in the concave region of the Pareto front. In CP, the utility function is usually defined as the minimum distance between the Pareto optimum to be sought and the utopia optimum or a reference point. Chen *et al*. (1999) developed a degenerated version of the CP method and modified the utility function into a max–min formulation. In heuristic hypermutation $\boldsymbol{T}^H(*)$, a CP method with the max–min formulation is used to guide the direction of mutation. More specifically, each antibody ($\mathbf{X}_j$) performs HSJ operation to maximize the following objective function:

$$\max U\left(\mathbf{X}_j\right) = \max\left(\min_{1\le i\le k}\left(w_i^j f_i\left(\mathbf{X}_j\right)\right)\right) \quad \text{subject to} \sum_i w_i^j = 1 \wedge w_i^j > 0 \tag{14}$$

It should be noticed that after the mutation, the utility of the mutated antibody $U\left(\mathbf{X}'_j\right)$ would be greater than that of the original antibody $U\left(\mathbf{X}_j\right)$. Therefore, we will have $\min\left(f_i\left(\mathbf{X}_j\right)\right) < \min\left(f_i\left(\mathbf{X}'_j\right)\right)$. According to the definition of *domination* in Equation (10), the mutated antibody $\mathbf{X}'_j$ will dominate the previous one. When maximizing the utility function's value C, the isolines of $\min_{1\le i\le k}\left(w_i^j f_i\left(\mathbf{X}_j\right)\right) = C$ will move towards the upper right region of the objective space. Since the coordinates of the isoline's lower left corner is $\left(C\big/w_1^j, C\big/w_2^j, \cdots, C\big/w_k^j\right)$, as the utility value C becomes larger, the

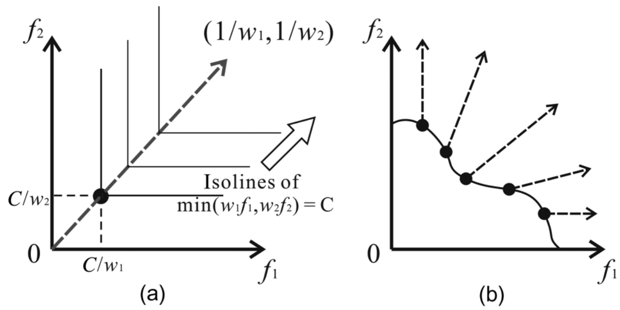

Figure 2. Heuristic hypermutation: (a) the isoline of the utility function, and (b) the searching directions of different antibodies.

moving direction of the isoline is a vector from the origin $(0, 0, \cdots, 0)$ to the reciprocal weights $\left(1\big/w_1^j, 1\big/w_2^j, \cdots, 1\big/w_k^j\right)$ (a bi-objective case is shown in Figure 2a). During the mutation, the larger is $1\big/w_i^j$, the more significant is f_i.

To assure the dispersion of the new antibody, directions of these single objectives are adjusted according to the distribution of the current population (Figure 2b). The weight corresponds to the ith objective of the jth antibody and is given by

$$\frac{1}{w_i^j} = \frac{f_i\left(\mathbf{X}_j\right) - f_i^{\min}}{f_i^{\max} - f_i^{\min}} \tag{15}$$

where

$$\begin{cases} f_i^{\max} = \max\limits_{\mathbf{X} \in \mathbf{B}} f_i\left(\mathbf{X}\right) \\ f_i^{\min} = \min\limits_{\mathbf{X} \in \mathbf{B}} f_i\left(\mathbf{X}\right) \end{cases} \tag{16}$$

In the above equation, $f_i^{\max}$ and $f_i^{\min}$, respectively, represent the maximum and minimum values of the ith objective of the solutions. For a solution with higher value of $f_i\left(\mathbf{X}\right)$, there is higher possibility for it to further improve on the corresponding objective. According to Equation (15), each antibody is made to pay more attention to its relatively advantageous objective by adjusting the searching direction. Moreover, such adjustment, shown in Figure 2b, also diverses the antibody population and potentially improves the evenness of the generated Pareto alternatives.

A key parameter for the operator $\boldsymbol{T}^H(*)$ is the mutation proportion p_m. For each antibody $(\mathbf{X}_j)$, the mutation is performed on $m = p_m \times R \times C$ pairs of cells, where the size of the study area is $R \times C$.

It should be noticed that there are only m times of comparisons to be performed for each antibody each iteration in the hypermutation operator. On the other hand, when applying dominance as accepting criterion in HSJ, the number of comparisons will rise up to $m \times (|B| - 1)$. That is because determining the state of dominance requires comparisons between the mutated antibody and every other one in the population. When dealing with regions with large area, m could be very large, and the multiplier $(|B| - 1)$ will result in an even heavier computation burden. Therefore, the proposed hypermutation operator is more efficient than conventional mutation, especially when applying in large-area regions.

3.2. Proportional cloning according to non-dominated neighbour

The proportional cloning operator $\mathbf{T}^C(*)$ on the dominant population $\mathbf{D} = \{\mathbf{X}_1, \mathbf{X}_2, \ldots, \mathbf{X}_{|\mathbf{D}|}\}$ is defined as

$$\begin{aligned}\mathbf{T}^C(\mathbf{D}) &= \left\{\mathbf{T}^C(\mathbf{X}_1), \mathbf{T}^C(\mathbf{X}_2), \ldots, \mathbf{T}^C\left(\mathbf{X}_{|\mathbf{D}|}\right)\right\} \\ &= \left\{\left\{\mathbf{X}_1^1, \mathbf{X}_1^2, \ldots, \mathbf{X}_1^{q_1}\right\}, \left\{\mathbf{X}_2^1, \mathbf{X}_2^2, \ldots, \mathbf{X}_2^{q_2}\right\} \ldots, \left\{\mathbf{X}_{|\mathbf{D}|}^1, \mathbf{X}_{|\mathbf{D}|}^2 \ldots, \mathbf{X}_{|\mathbf{D}|}^{q_{|\mathbf{D}|}}\right\}\right\}\end{aligned} \tag{17}$$

In the immune system, cloning is the asexual propagation of the antibody, which reproduces offspring identical to the ancestor. Usually, the amount of cloned offspring q_i is proportional to the parent's affinities. Using proportional cloning, we aim to make AIS-MOLA pay more attention to the less crowded region in objective space. Such crowding criterion can be measured by a metric known as crowding distance (Deb *et al.* 2000). Therefore, this metric is used to quantify the affinity in AIS-MOLA (illustrated in Figure 3):

$$\zeta(\mathbf{X}, \mathbf{D}) = \sum_{i=1}^{k} \frac{\zeta_i(\mathbf{X}, \mathbf{D})}{f_i^{\max} - f_i^{\min}} \tag{18}$$

where $f_i^{\max}$ and $f_i^{\min}$ have the same meaning as in Equation (16), and the ith crowding distance is

$$\zeta_i(\mathbf{X}, \mathbf{D}) \begin{cases} \infty, f_i(\mathbf{X}) = \min\{f_i(\mathbf{X}_1) \,|\mathbf{X}_1 \in \mathbf{D}\} \; or \; f_i(\mathbf{X}_2) = \max\{f_i(\mathbf{X}_2) \,|\mathbf{X}_2 \in \mathbf{D}\} \\ \min\{f_i(\mathbf{X}_1) - f_i(\mathbf{X}_2) \,|\mathbf{X}_1, \mathbf{X}_2 \in \mathbf{D} : f_i(\mathbf{X}_1) < f_i(\mathbf{X}) < f_i(\mathbf{X}_2)\}, \text{otherwise} \end{cases} \tag{19}$$

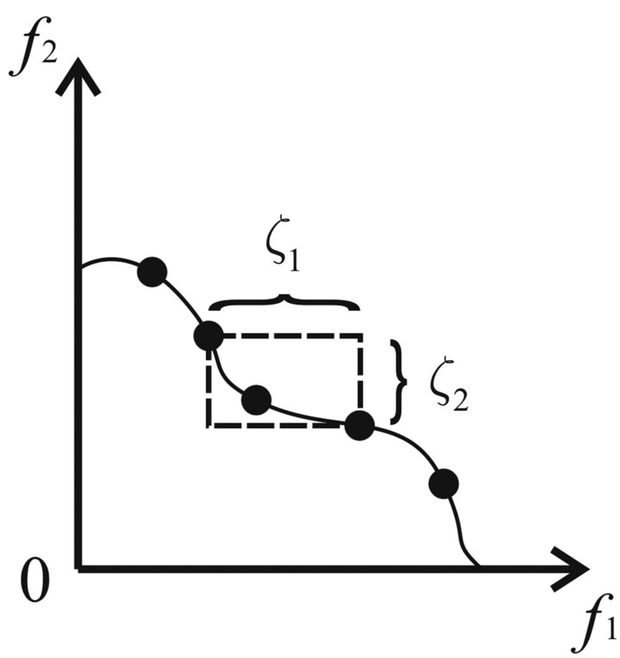

Figure 3. The illustration of crowding distance in the two-dimensional objective space.

Crowding distance with infinity value is set to the double of the maximum value of the remaining antibodies. Then, the amount of offspring cloned from antibody $\mathbf{X}_i$ is calculated by

$$q_i = \left\lceil n_C \times \frac{\zeta\left(\mathbf{X}_i, \mathbf{D}\right)}{\sum_{j=1}^{|\mathbf{D}|} \zeta\left(\mathbf{X}_j, \mathbf{D}\right)} \right\rceil \tag{20}$$

where n_C is the expected size of clone population $\mathbf{C}$ and $\lceil * \rceil$denotes the ceiling function.

3.3. Recombination strategy preserving connected land-use patches

The recombination operator $\mathbf{T}^R$ between cloning population $\mathbf{C} = \left\{\mathbf{X}_1, \mathbf{X}_2, \ldots, \mathbf{X}_{|\mathbf{C}|}\right\}$ and dominant population $\mathbf{D}$ is defined as

$$\begin{aligned} \mathbf{T}^R\left(\mathbf{C}, \mathbf{D}\right) &= \left\{\mathbf{T}^R\left(\mathbf{X}_1, \mathbf{D}\right), \mathbf{T}^R\left(\mathbf{X}_2, \mathbf{D}\right), \ldots, \mathbf{T}^R\left(\mathbf{X}_{|\mathbf{C}|}, \mathbf{D}\right)\right\} \\ &= \left\{\text{crossover}\left(\mathbf{X}_1, \mathbf{D}\right), \text{crossover}\left(\mathbf{X}_2, \mathbf{D}\right), \ldots, \text{crossover}\left(\mathbf{X}_{|\mathbf{C}|}, \mathbf{D}\right)\right\} \end{aligned} \tag{21}$$

where crossover $(\mathbf{X}_i, \mathbf{D})$ denotes generating 'offspring', that is, new solutions, by combining the advantages of two 'parents', that is, the cloned antibody $\mathbf{X}_i$ and one individual equiprobably selected from $\mathbf{D}$.

Such *crossover* operation is widely used in evolutionary computation. Conventionally, this operation is carried out by randomly splitting each parent into two parts, and then constructing the offspring with one part of each parent. In land-use allocation, this splitting may violate the area constraints in Equation (3) because the split parts may contain different proportions of land use. To avoid the violation, Wu *et al*. (2011) integrated greedy heuristic to repair the generated offspring. However, this repair brings about additional computation burden, and is thus inefficient when applied in a problem with large area. To resolve the same problem, Stewart *et al*. (2004) proposed a crossover operator that only takes into account the regions with different land uses in two parents. It first identifies all these regions and then allocates randomly one kind of land use to each half of these cells. Although Stewart's *crossover* operator manages to preserve the area constraints, the resulting offspring tend to be highly fragmented because the random allocation does not take into account the conjunction between cells. In accordance with the same principle of preserving area constraints, we try to resolve the fragmentation issue by assigning connected patches rather than isolated cells.

Suppose there are two allocation solutions $\mathbf{X}_1$ and $\mathbf{X}_2$. For each pair of land uses, say k_l and k_m, a land-use change detection technique is used to identify all cells where land use is k_l in one parent ($\mathbf{X}_1$) and k_m in the other ($\mathbf{X}_2$). When there are K kinds of land uses, then there are K^2 kinds of cells identified. Each of them can be represented as

$$\mathbf{W}\left(k_l, k_m\right) = \left\{(i,j) \,|\mathbf{X}\left(i,j,k_l\right) = 1 \wedge \mathbf{X}\left(i,j,k_m\right) = 1\right\} \tag{22}$$

Every set of $\mathbf{W}\left(k_l, k_m\right)$ is then split into connected patches by area fill algorithms in computer graphics (e.g. seed fill algorithm and scan line fill algorithm) (Heare and Baker 1998):

$$\mathbf{W}\left(k_l, k_m\right) = w^1\left(k_l, k_m\right) \cup w^2\left(k_l, k_m\right) \cup \cdots \cup w^{n_{k_l k_m}}\left(k_l, k_m\right) \tag{23}$$

In the offspring solution $\mathbf{X}^*$, the land use of each connected patch is randomly inherent from one of its parents. This procedure continues until we reach the very patch that, if assigned, the area constraint will be violated. This particular land-use patch is then split into two smaller patches to satisfy that constraint. By assigning connected patches rather than isolated cells, the proposed *crossover* operator can reduce the influence of fragmentation issue as much as possible.

A simple example, with a region of 6×6 grid is used to illustrate the *crossover* operator. Three types of land uses are convertible in this example, with each of them occupying an area with 12 cells. Figure 4 shows the detailed procedure of the *crossover* operator step by step. Note that by considering connected patches and maintaining area proportions, the

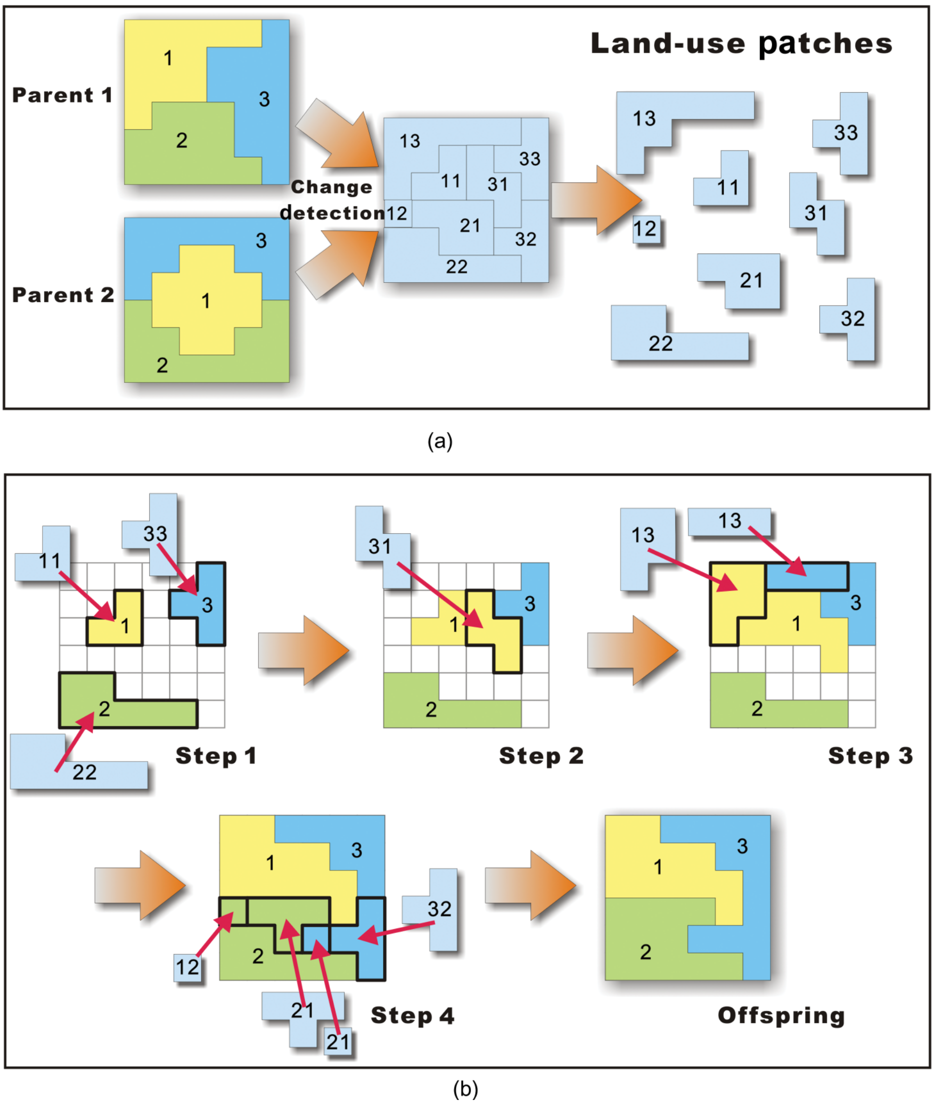

Figure 4. A simple example to illustrate the crossover operator: (a) change detection and (b) offspring construction.

proposed crossover operator is also potentially useful in the aforementioned EAs for land allocation. In that, this crossover operator may be able to enhance their performance when applying in large-area regions or area constraints are restricted.

4. Implementation and results

Two experiments were performed on AIS-MOLA. One is validated by a hypothetical land-use allocation problem and the other is applied in a real-world MLUA (multisite land use allocation) problem in Panyu. The former experiment validates whether AIS-MOLA is capable of approximating the Pareto front of MLUA, whereas the latter one shows the applicability of this algorithm in a real-world application.

The proposed algorithm was implemented using Visual C#. All experiments were run on a PC with Intel (R) Core (TM) 2, 2.33 GHz CPU, 2.00 GB RAM and Windows 7 OS. Moreover, a free version of AIS-MOLA can be downloaded from http://www.geosimulation.cn/AIS-MOLA/, including all the data sets used in the experiments.

4.1. Validation using hypothetical data

In this subsection, we aim to validate whether the alternatives generated by AIS-MOLA are distributed evenly over the Pareto front, which is one of the overriding concerns about the algorithm's performance. However, this validation may be disturbed by the spatial autocorrelation (Goodchild 1988) of geographic phenomenon. Considering the spatial autocorrelation issue, land-use patterns with high suitability tend to have relatively high compactness as well. The Pareto alternatives of a real-world land-use allocation problem probably distribute around a narrow region in objective space. As a result, AIS-MOLA should be validated by a hypothetical land allocation problem involving limited spatial autocorrelation.

The hypothetical problem asks the planner to allocate four types of land use, aiming to optimize the spatial suitability and the compactness described in Section 2.1. Each of these land uses occupies 25% of the study region. We reduced the influence of spatial autocorrelation by setting the suitability layers to a random number between [0,1] (Figure 5). The corresponding Moran's index, Z-score and P-value of each suitability layer are listed in Table 1. Note that all of the Moran's indices are very close to zero, which indicates that the degree of spatial autocorrelation is negligible. By reducing this influence of spatial autocorrelation, all possible solutions will spread around a wide region, and the true Pareto front should form a curve from (1,0) to (0,1).

Besides the validation, we further compared the performances of AIS-MOLA and another approach (Duh and Brown 2007) that utilized PSA (Czyzak and Jaszkiewicz 1998), which is referred to as PSA-MOLA. As is discussed in Section 1, PSA-MOLA can handle grid-represented land-use allocation problems with area constraints as the proposed method concerned. The same objective, to generate Pareto optimal alternatives in land-use allocation problems represented by grids, makes PSA-MOLA the most comparable approach with AIS-MOLA. In addition, Simulated Annealing (SA) algorithm is an important baseline method for land-use allocation, which has been used as a standard for comparison in several other literatures (Chen *et al.* 2010, Li *et al.* 2010, Liu *et al.* 2012). PSA is conceptually identical to the conventional SA (Czyzak and Jaszkiewicz 1998), which simulates the cooling process of materials in a heat bath. SA is essentially a random local search method that accepts improved solutions with higher probability and deteriorated ones with a lower probability. During the annealing process, the probability of

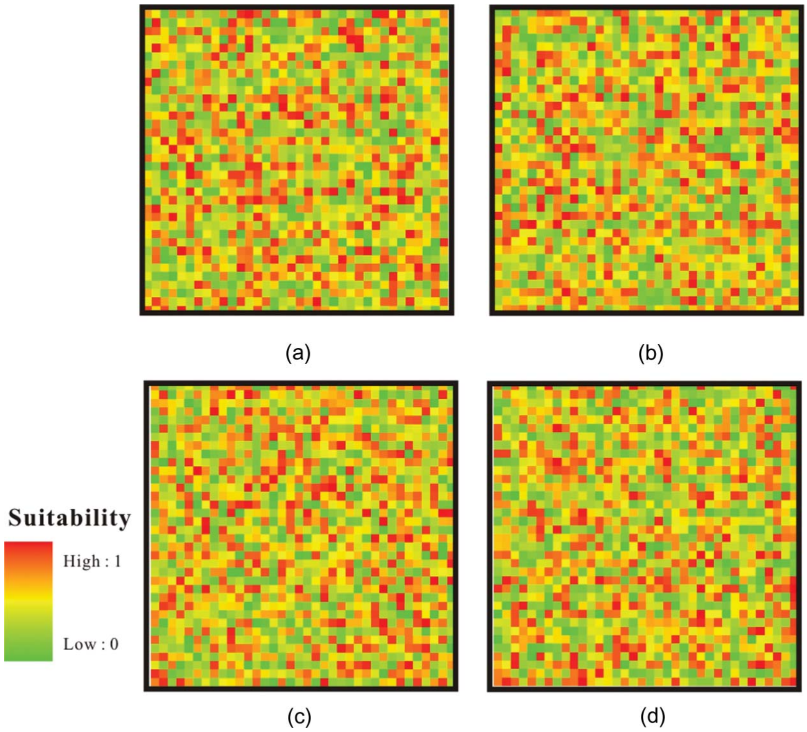

Figure 5. Spatial suitability for 4 types of land use in the hypothetical problem: (a), (b), (c), and (d) represent Land-use type-1, -2, -3 and -4, respectively.

Table 1. Spatial autocorrelation of the suitability layers in the hypothetical problem.

Suitability layer	Moran's index	*Z*-score	*P*-value
Land-use type-1	−0.001318	0.014039	0.988799
Land-use type-2	0.023381	0.896668	0.402779
Land-use type-3	0.005776	0.250301	0.802354
Land-use type-4	−0.066176	−2.146237	0.031854

accepting deteriorations decreases as the temperature drops. PSA seeks the Pareto optimal alternatives via a modified schema of SA. Instead of altering one solution and optimizing a single objective, PSA uses a set of interaction solutions as annealing status and several weighted objectives as an acceptance criterion.

For the sake of a fair comparison, these two algorithms are implemented on the same platform and share a series of common codes. Both the local search in PSA-MOLA and the mutation in AIS-MOLA are based on the HSJ technique and share the same set of codes. Moreover, they also share the same procedures and code for dominant determination and objective evaluations.

The parameters set for these algorithms and runtimes are listed in Table 2. The meaning of the parameters of AIS-MOLA is described in Section 3. In PSA-MOLA, initial temperature and dispersion factor play key roles. If the initial temperature is too high, then the algorithm will take too much time to converge. If the initial temperature is too low,

Table 2. Parameters and runtimes of AIS-MOLA and PSA-MOLA.

AIS-MOLA		PSA-MOLA	
Size of population	50	Size of generating set	50
Number of generations	300	Number of iterations	3000
Cloning proportion	30%	Initial temperature	0.05
Mutation proportion	30%	Dispersion factor	1.1
Runtime (hh:mm:ss)	00:02:44	Runtime (hh:mm:ss)	01:05:58

then the algorithm will be easily trapped in the local optimal. The dispersion factor, on the other hand, determines the way PSA adjusts the associated weight of every objective. This adjusting mechanism assures the dispersion of the generated solutions in objective space. Usually, the dispersion factor is set as a constant greater than one.

The Pareto solutions generated by these two approaches are plotted in Figure 6, and the spatial patterns of eight labelled solutions are shown in Figure 7. All solutions generated by AIS-MOLA *dominate* those generated by PSA-MOLA, which suggests that the former solutions can better approximate the true Pareto front. Although AIS-MOLA generates better solutions, it takes only 1/20 of the runtime of PSA-MOLA (runtime is listed in Table 1). The efficiency of AIS-MOLA indicates its potential for implementation in large-area land-use allocations.

4.2. Application in study area

In addition to the validation, the proposed algorithm was applied to the land-use allocation problem of Panyu City, PR China. This case study aims to allocate four types of land

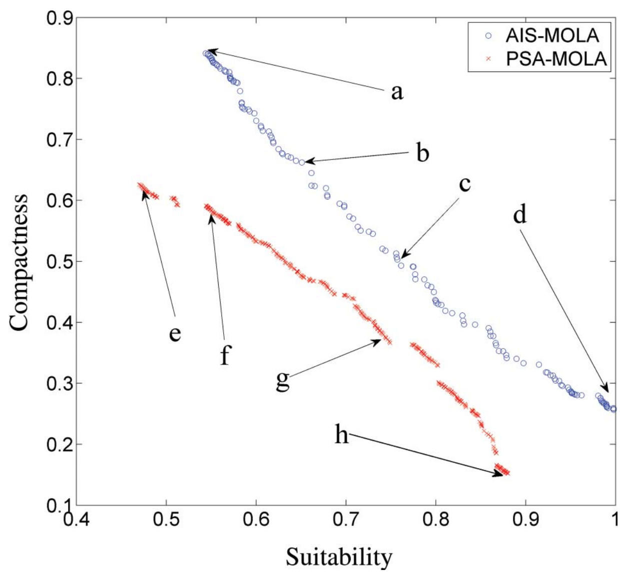

Figure 6. The Pareto front generated by AIS-MOLA and PSA-MOLA: (a)–(d) are 4 solutions generated by AIS-MOLA, and (e)–(h) are 4 solutions generated by PSA-MOLA.

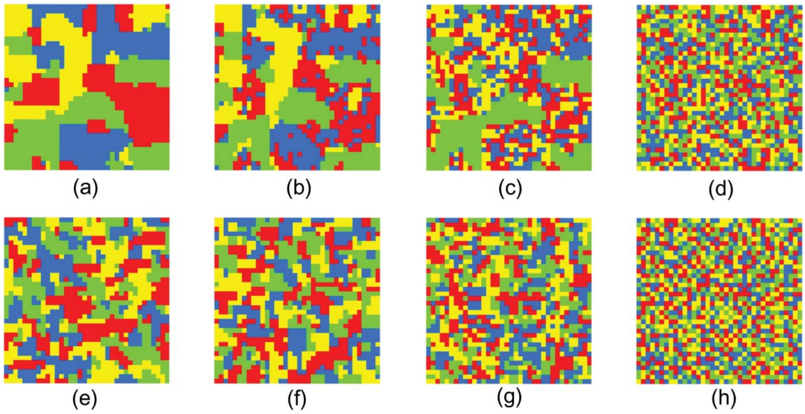

Figure 7. Corresponding spatial patterns of the labelled solutions in Figure 6.

uses (agriculture, industry, commerce and residence), optimizing two planning objectives (maximizing land-use suitability and compactness).

4.2.1. Study area and objectives

Panyu has an area of 786 km^2, located at the centre of the Pearl River Delta (PRD) in Guangdong Province (Figure 8). Since the 1980s, fast economic development and rapid urban sprawl have been witnessed in the PRD region, thanks to the implementation of

Figure 8. The location of the study area.

the Reform and Opening-Up Policy. As the transportation junction between the biggest cities in the PRD, Panyu has attracted large quantities of factories and residents. This mass movement raised the demands on land use for industry, residence and commerce, as well as caused a large amount of agricultural land loss. This issue has resulted to serious conflicts between multiple types of land uses because many regions may be suitable for several different land uses. Simply allocating land use to the most suitable sites inevitably results in a fragmented land-use pattern. To adjust the balance between spatial suitability and compactness, we applied the AIS-MOLA algorithm to generate Pareto alternatives that can reveal the trade-off between them.

The study area is represented as a two-dimensional grid with 389×337 cells. There are eight kinds of land uses in this area, including agriculture, industry, commerce, residence, wildness, water, forest and roads. Only four land uses (agriculture, industry, commerce and residence) are convertible in this study because of the difficulty of converting others. The required areas for four types of allocable land uses are listed in Table 3. In all, there are 62,917 allocable cells, which result in $4^{62917} \approx 6.44 \times 10^{37879}$ candidate solutions to the planning problem.

The goal of this study was to optimize those two planning objectives – spatial suitability and compactness. Considering various different factors and objectives involved in the definition of spatial suitability, a very high-dimensional objective space may be confronted with when directly taking into account all the relative factors. MOPs with high-dimensional objective space may become intractable, since even the performance of those well-established MOP algorithms degrades as the number of objectives increases (Khare 2002, Ishibuchi *et al.* 2008). One possible solution for this issue is to obtain the spatial suitability by taking the linear weighted sum of these factors (Eastman *et al*. 1998, Malczewski 1999) whose associated weights are derived by analytic hierarchy process (AHP) (Saaty 1990). AHP can determine the relative importance among complex factors by incorporating experiences of experts and performing pairwise comparisons. The derived weights of 14 factors for each land-use type are listed in Table 4, and the resulting spatial suitability for each land-use type is shown in Figure 9.

Linear weighted summation as a dimension reduction technique for spatial suitability derivation, however, is not suitable for further combining the two planning objectives – spatial suitability and compactness. That is because of the disparate nature of these two objectives: the spatial suitability is site-related, whereas the spatial compactness is aggregation-related. Additionally, in AHP, experts must determine each factor's relative importance, which is difficult to obtain when dealing with two disparate objectives.

As can be seen from Figure 9, the spatial suitability of real-world land-use allocation problems is with a relatively higher degree of spatial autocorrelation than the hypothetical problem mentioned in Section 4.1. Each suitability layer's corresponding Moran's index, Z-score and P-value were calculated and are listed in Table 5. The very high Z-scores

Table 3. Allocation amount for the four land uses.

Land-use type	Area (km^2)	Number of rasters
Agriculture	27.389	27,389
Industry	9.74	9741
Commerce	6.33	6334
Residence	16.73	16,727

Table 4. Weights of factors for each of the four land uses. These weights are a dimensionless number.

Factors	Agriculture	Industry	Commerce	Residence
NDVI (normalized difference vegetation index)	0.1385	N/A	N/A	N/A
Slope	0.0965	0.1253	0.1266	0.1124
Elevation	0.1097	0.0867	0.0935	0.0827
Fertility	0.2353	N/A	N/A	N/A
pH value of soil	0.1598	N/A	N/A	N/A
Geological disaster potential	N/A	0.1427	0.1461	0.1479
Distance to towns	0.0653	0.0675	0.1251	0.1029
Distance to highways	0.0467	0.1669	0.0528	0.0764
Distance to roads	0.0585	0.1553	0.1035	0.0886
Density of green surfaces	N/A	0.0286	0.0297	0.0923
Proximity to river	0.0897	0.0254	0.0169	0.0227
Proximity to industry	N/A	0.1622	0.0135	0.0119
Proximity to commerce	N/A	0.0236	0.1753	0.1054
Proximity to residence	N/A	0.0108	0.1170	0.1568
Sum	1	1	1	1

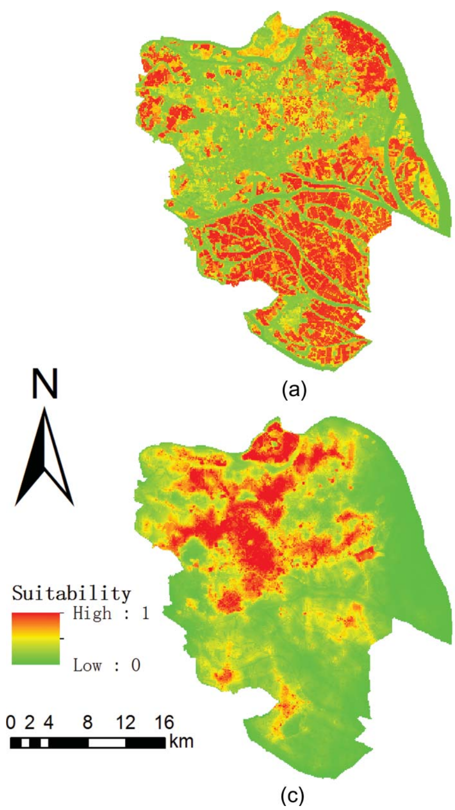

Figure 9. Spatial suitability of the four land uses: (a)-Agriculture, (b)-Industry, (c)-Commerce, (d)-Residence.

Table 5. Spatial autocorrelation of the suitability layers in the study area.

Suitability layer	Moran's index	*Z*-score	*P*-value
Agriculture	0.801174	437.600718	0
Industry	0.897737	524.420595	0
Commerce	0.959976	504.246475	0
Residence	0.923033	490.43727	0

associated with very small *P*-values indicate that the indices of spatial autocorrelation are credible. By simply maximizing the spatial suitability, one may be able to generate a land-use allocation solution with a higher degree of compactness in real world than in a hypothetical problem. However, previous studies (Chen *et al.* 2010, Li *et al.* 2010) showed that land-use allocation in real-world application without considering contiguity constraint will result in a fragmented pattern, which is difficult to manage. By approximating the true Pareto front of this problem, we hope to discover the trade-off between spatial suitability and compactness in this area.

4.2.2. Implementation and results

As a result of the enormous amount of possible solutions, AIS-MOLA took about 1 hour and 20 minutes to converge and generate the resulting Pareto alternatives. The images of these alternates in objective space are shown in Figure 10. Among them, the spatial patterns of four labelled solutions are shown in Figure 11. As can be seen in Figure 10, solution (d) has the highest suitability and the corresponding spatial pattern is very fragmented. On the other hand, solution (a) has the highest compactness. The corresponding spatial pattern has many connected patches.

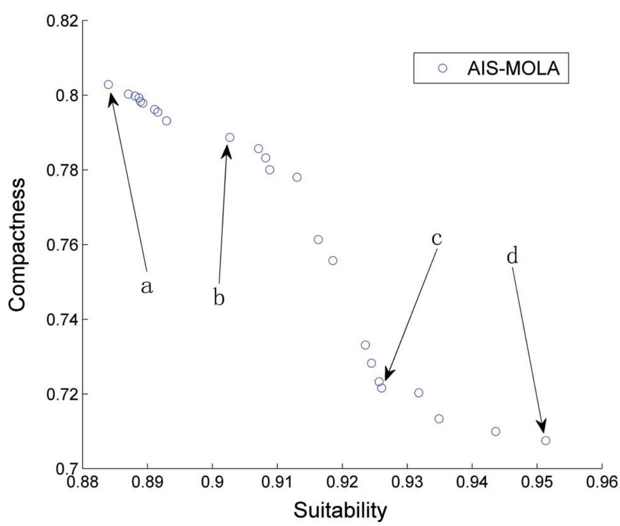

Figure 10. Pareto alternatives of MLUA problem of PanyuCity generated by AIS-MOLA: (a)–(d) are 4 selected solutions, whose corresponding spatial patterns are shown in Figure 11.

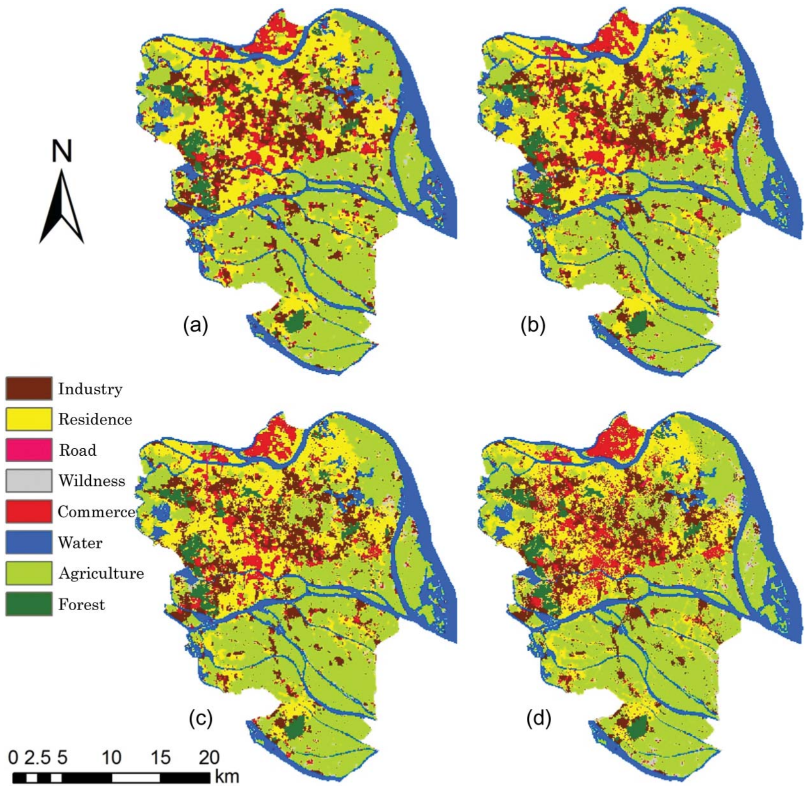

Figure 11. Corresponding spatial patterns of the labelled solutions in Figure 10: (a)–(d) are the spatial patterns of the solutions labelled by (a)–(d) in Figure 10, respectively.

Whereas it is very difficult, or even impossible, to validate the resulting Pareto alternatives by comparing them with the true Pareto front, especially for such multi-objective problems with high-dimensional solution space, one possible way for validation is to approximately sample the Pareto front by single-objective optimization techniques. Recently, a multi-type ant colony optimization method for multiple land allocation (MACO-MLA) model (Liu *et al.* 2012) has been proposed to solve the single-objective land allocation in large area. The proposed MACO-MLA model has indicated that it can yield better performances than the SA and GA methods. To validate the resulting alternatives, we applied MACO-MLA in the study area, with different combinations of sub-objective weights listed in Table 6. The solutions generated by AIS-MOLA and

Table 6. Different sets of sub-objective weights used in MACO-MLA optimization and the corresponding results. The weights of different objectives are a dimensionless number.

Label	Weight of suitability	Weight of compactness	Suitability	Compactness
I	0.25	0.75	0.84501	0.80063
II	0.50	0.50	0.89819	0.79118
III	0.75	0.25	0.92320	0.75225
IV	0.85	0.15	0.92985	0.72951
V	1.00	0.00	0.94853	0.71865

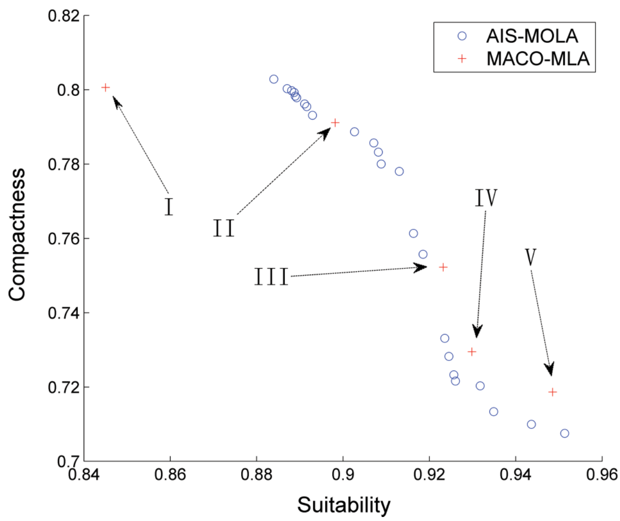

Figure 12. Solutions generated by AIS-MOLA (blue circles) and MACO-MLA (red crosses): I–V are 5 solutions generated by MACO-MLA algorithm.

MACO-MLA are plotted in Figure 12. As can be seen from this figure, although some solutions generated by AIS-MOLA are inferior to those generated by MACO-MLA, the former ones can provide reasonable approximation for the latter ones.

Further insight into the shape of the Pareto front in Figure 10 shows its value for land-use planning decision-makers. According to the distribution of the Pareto alternatives, we can infer that under different circumstances, the improvement of one objective may result in different degrees of deterioration on the other objectives. For instance, from solutions (d) to (c), the decrease in suitability does not bring too much increase in compactness, whereas from solutions (c) to (b), the same amount of decrease in suitability leads to great improvement in compactness. However, from solutions (b) to (a), a further decrease in suitability makes limited a contribution to compactness. To sum up, the shape of the Pareto front tells decision-makers how much is needed to scarify when purchasing a particular planning objective.

In real-world land-use planning applications, relations between different objectives can be very complex. If we simplify a multi-objective problem into a single-objective problem, a decision-maker will never be aware whether he has sacrificed too much on some objectives for a tiny increase on one objective. The approximate Pareto front generated by AIS-MOLA helps decision-makers analyse the complex trade-off between different objectives, which could help improve the reliability of decision-making.

5. Conclusion

In this article, we focus on the grid-represented land-use allocation problem, in which the shapes of land-use patches need to be optimized and the area proportions need to be maintained. Specifically, we aim to solve such problems with multiple objectives and in large area. AIS has been utilized when attempting to achieve this goal, because previous researches (Coello and Cortés 2005, Jiao *et al.* 2005, Gong *et al*. 2008) have indicated that AIS has the potential of solving high-dimensional multi-objective problems more efficiently. Moreover, we have developed an improved AIS algorithm for MOLA (AIS-MOLA) and modified the basic immunological operators. The three modified operators equipped by the proposed algorithms include (1) a heuristic hypermutation based on CP, (2) a non-dominated neighbour-based proportional cloning and (3) a novel crossover operator that preserves connected patches. These modifications make AIS more suitable for grid-represented land allocation problem, as well as further improve its efficiency in the case of large-area regions. By developing AIS-MOLA, we managed to generate Pareto alternatives of MOLA problems in large-area regions.

The proposed algorithm has been validated by a small-area hypothetical land-use allocation problem with low spatial autocorrelation. Meanwhile, during the validation, its performance and efficiency were compared with PSA-MOLA. The comparison shows that AIS-MOLA can generate solutions that are more approximate to the true Pareto front. Furthermore, AIS-MOLA spends only 1/20 of the runtime of PSA-MOLA. The satisfactory performance and the efficiency of AIS-MOLA indicate its potential of implementation in large-area MOLA problems. After validation, AIS-MOLA was applied in a case study of Panyu City. This application allocated four types of land uses and simultaneously optimized two planning objectives. The study area was represented as a two-dimensional grid with 62,917 allocable cells, which means that there were approximately $4^{62917} \approx 6.44 \times 10^{37879}$ possible solutions. Although dealing with a land-use allocation problem with huge solution space, AIS-MOLA generated satisfactory Pareto alternatives within an acceptable computation time of about 1 hour and 20 minutes. In addition, further insights into the generated Pareto front inform us that under different circumstances, the same amount of improvement on spatial suitability will result in different amounts of deterioration on spatial compactness. Hence, the distribution of these alternatives can quantitatively demonstrate the trade-offs between suitability and compactness of land use in Panyu City, which should provide valuable information for land-use planning decision.

For simplicity and better visualization, only two planning objectives – the spatial suitability and compactness – were considered in this study. The two planning objectives and the suitability layers derived by AHP are merely inputs of the proposed algorithm, and therefore the determination of objective and suitability is independent to the efficacy of the presented methodology. In other words, if more reasonable suitability layers are given or other more realistic planning objectives are defined, AIS-MOLA can generate Pareto alternatives in large-area regions as well. However, the applications of this algorithm should not be limited to these objectives. As described in Section 3, the procedure of AIS-MOLA only requires grid representation and quantifiable objectives. The implementations of the modified immunological operators are not restricted by definitions of the objective functions. Therefore, theoretically, this approach can be applied to the optimization for other planning objectives.

Nevertheless, since MOPs with many objectives are still intractable even for those well-established MOP algorithms, most MOLA methods can only handle two or three planning objectives (e.g. the approaches proposed by Matthews (2001), Bennett *et al*. (2004), Roberts *et al.* (2011), Cao *et al.* (2011) and Duh and Brown (2007)). Such limitation is also shared by AIS-MOLA. In the future studies, its capability of handling more than three or four objectives will be further verified and improved. Additionally, our future study will take into account the planning objectives in other forms, such as cost of land-use conversion and spatial consistency and spatial proximity of different types of land use. Moreover, land-use planning may involve more complicated goals, for example, minimizing traffic jams and pollutants and maximizing economic productivity and utility of public facilities. Before applying the land-use planning algorithm, planners have to define some reasonable objective functions that can appropriately reflect and quantify those planning objectives. As a result, the definitions of more realistic and pragmatic objective functions should also be further included in future studies. A more user-friendly programme should be developed to provide such flexibility in dealing with various objectives.

Acknowledgements

This study was supported by the National Natural Science Foundation of China (Grant Nos. 41171308 and 40901187) and the Key National Natural Science Foundation of China (Grant No. 40830532).

References

Aerts, J.C.J.H. and Heuvelink, G.B.M., 2002. Using simulated annealing for resource allocation. *International Journal of Geographical Information Science*, 16 (6), 571–587.

Aerts, J.C.J.H., *et al*., 2003. Using linear integer programming for multi-site land-use allocation. *Geographical Analysis*, 35 (2), 148–169.

Bennett, *et al*., 2004. Exploring the geographic consequences of public policies using evolutionary algorithms. *Annals of the Association of American Geographers*, 94, 827–847.

Brill, E.D., Chang, S.Y., and Hopkins, L.D., 1982. Modeling to generate alternatives: the HSJ approach and an illustration using a problem in land use planning. *Management Science*, 28 (3), 221–235.

Brill Jr., E.D., *et al*., 1990. MGA: a decision support system for complex, incompletely defined problems. *IEEE Transactions on Systems, Man and Cybernetics*, 20 (4), 745–757.

Brookes, C.J., 2001. A genetic algorithm for designing optimal patch configurations in GIS. *International Journal of Geographic Information Science*, 15 (6), 539–559.

Campbell, J., *et al*., 1992. An application of linear programming and geographic information systems: cropland allocation in Antigua. *Environment and Planning A*, 24 (4), 535–549.

Cao, K., *et al*., 2011. Spatial multi-objective land use optimization: extensions to the non-dominated sorting genetic algorithm-II. *International Journal of Geographical Information Science*, 25 (12), 1949–1969.

Chen, W., Wiecek, M.M., and Zhang, J., 1999. Quality utility – a compromise programming approach to robust design. *Journal of Mechanical Design*, 121, 179–187.

Chen, Y., *et al*., 2010. An agent-based model for optimal land allocation (AgentLA) with a contiguity constraint. *International Journal of Geographical Information Science*, 24 (8), 1269–1288.

Coello, C.A.C. and Cortés, N.C., 2005. Solving multiobjective optimization problems using an artificial immune system. *Genetic Programming and Evolvable Machines*, 6 (2), 163–190.

Coello, C.A.C., Pulido, G.T., and Lechuga, M.S., 2004. Handling multiple objectives with particle swarm optimization. *IEEE Transactions on Evolutionary Computation*, 8 (3), 256–279.

Cova, T.J. and Church, R.L., 2000. Exploratory spatial optimization in site search: a neighborhood operator approach. *Computers & Operations Research*, 24, 401–419.

Crohn, D.M. and Thomas, A.C., 1998. Mixed-integer programming approach for designing land application systems at a regional scale. *Journal of Environmental Engineering*, 124, 170.

Czyzak, P. and Jaszkiewicz, A., 1998. Pareto simulated annealing – A metaheuristic technique for multiple-objective combinatorial optimization. *Journal of Multi-Criteria Decision Analysis*, 7, 34–47.

Das, I. and Dennis, J., 1997. A closer look at drawbacks of minimizing weighted sums of objectives for Pareto set generation in multicriteria optimization problems. *Structural and Multidisciplinary Optimization*, 14 (1), 63–69.

Dasgupta, D. and Nino, F., 2008. *Immunological computation: theory and applications*. Boca Raton, Florida: Auerbach Publications.

Deb, K., 2001. *Multi-objective optimization using evolutionary algorithms*. London: John Wiley & Sons.

Deb, K., *et al*., 2000. A fast elitist non-dominated sorting genetic algorithm for multi-objective optimization: NSGA-II. *Lecture Notes in Computer Science*, 1917, 849–858.

Duh, J.-D. and Brown, D.G., 2007. Knowledge-informed Pareto simulated annealing for multi-objective spatial allocation. *Computers, Environment and Urban Systems*, 31 (3), 253–281.

Eastman, J.R., Jiang, H., and Toledano, J., 1998. Multi-criteria and multi-objective decision making for land allocation using GIS. *Environment and Management*, 9, 227–252.

Eldrandaly, K., 2010. A GEP-based spatial decision support system for multisite land use allocation. *Applied Soft Computing*, 10 (3), 694–702.

Garrett, S.M., 2005. How do we evaluate artificial immune systems? *Evolutionary Computation*, 13 (2), 145–177.

Gong, M.G., *et al*., 2008. Multiobjective immune algorithm with nondominated neighbor-based selection. *Evolutionary Computation*, 16 (2), 225–255.

Goodchild, M.F., 1988. *Spatial Autocorrelation*. Norwich: Geobooks.

Heare, D. and Baker, M.P., 1998. *Computer Graphics (C Version)*. New Jersey: Prentice Hall International Inc.

Hopkins, L., Brill Jr., E., and Wong, B., 1982. Generating alternative solutions for dynamic programing models of water resources problems. *Water Resources Research*, 18 (4), 782–790.

Huang, B., *et al*., 2008. Seeking the Pareto front for multiobjective spatial optimization problems. *International Journal of Geographical Information Science*, 22 (5), 507–526.

Ishibuchi, H., *et al*. 2008. Evolutionary many-objective optimization: A short review. In *Proceedings of 2008 IEEE Congress on Evolutionary Computation*, 2424–2431.

Jahn, J., Klose, J., and Merkel, A., 1991. On the application of a method of reference point approximation to bicriterial optimization problems in chemical engineering. *In*: W. Oettli and D. Pallaschke, (eds.) *Advances in Optimization*. Berlin, Heidelberg, New York: Springer, 478–491.

Jiao *et al*. 2005. Clonal selection with immune dominance and anergy based multiobjective optimization. *Lecture Notes in Computer Science*, 3410, 474–489.

Jones, D.F., *et al*., 2002. Multi-objective meta-heuristic: An overview of the current state-of-the-art. *European Journal of Operational Research*, 137 (1), 1–9.

Keeney, R.L. and Raiffa, H., 1993. *Decisions with multiple objectives: Preferences and value tradeoffs*. Cambridge, UK: Cambridge University Press.

Khare, V., 2002. *Performance scaling of multi-objective evolutionary algorithms*. Thesis. Indian Institute of Technology.

Knowles, J.D. and Corne, D.W., 2000. Approximating the non-dominated front using the Pareto archive evolutionary strategy. *Evolutionary Computation*, 8 (2), 149–172.

Koski, J., 1988. Multicriteria truss optimization. *Multicriteria Optimization in Engineering and in the Sciences*, 37, 263.

Li, X., *et al*., 2010. Coupling urban cellular automata with ant colony optimization for zoning protected natural areas under a changing landscape. *International Journal of Geographical Information Science*, 99999 (1), 1–19.

Ligmann-Zielinska, A., Church, R.L., and Jankowski, P., 2008. Spatial optimization as a generative technique for sustainable multiobjective land-use allocation. *International Journal of Geographical Information Science*, 22 (6), 601–622.

Liu, X.P., Li, X., and Zhang, X.H., 2010. Simulating land use dynamics under planning policies by integrating artificial immune systems with cellular automata. *International Journal of Geographic Information Science*, 24 (5), 783–802.

Liu, X.P., *et al*., 2011. Zoning farmland protection under spatial constraints by integrating remote sensing, GIS and artificial immune systems. *International Journal of Geographic Information Science*, 25 (11), 1829–1848.

Liu, X.P., *et al*., 2012. A multi-type ant colony optimization (MACO) method for optimal land use allocation in large areas. *International Journal of Geographical Information Science*, 26 (7), 1325–1343.

Malczewski, J., 1999. *GIS and multicriteria decision analysis*. New York, NY: Wiley.

Matthews, K.B., 2001. *Applying genetic algorithms to multi-objective land-use planning*. Thesis (PhD). The Robert Gordon University.

Nam, D. and Park, C.H., 2000. Multiobjective simulated annealing: a comparative study to evolutionary algorithms. *International Journal of Fuzzy Systems*, 2 (2), 87–97.

Pareto, V., 1971. *Manual of political economy*. New York: Macmillan.

Roberts, S., Hall, G., and Calamai, P., 2011. Evolutionary multi-objective optimization for landscape system design. *Journal of Geographical Systems*, 13 (3), 299–326.

Saaty, T.L., 1990. How to make a decision: the analytic hierarchy process. *European Journal of Operational Research*, 48 (1), 9–26.

Santé-Riveira, I., *et al*., 2008. Algorithm based on simulated annealing for land-use allocation. *Computers & Geosciences*, 34 (3), 259–268.
Siitonen, P., Tanskanen, A., and Lehtinen, A., 2003. Selecting forest reserves with a multiobjective spatial algorithm. *Environmental Science & Policy*, 6 (3), 301–309.
Srinivas, N. and Deb, K., 1994. Multi-objective optimization using non-dominated in genetic algorithms. *Evolutionary Computation*, 2 (3), 221–248.
Stewart, T.J., Janssen, R., and van Herwijnen, M., 2004. A genetic algorithm approach to multiobjective land use planning. *Computers & Operations Research*, 31 (14), 2293–2313.
Wu, X., Murray, A.T., and Xiao, N., 2011. A multiobjective evolutionary algorithm for optimizing spatial contiguity in reserve network design. *Landscape Ecology*, 26 (3), 425–437.
Youssef, H., Sait, S.M., and Adiche, H., 2001. Evolutionary algorithms, simulated annealing and tabu search: a comparative study. *Engineering Applications of Artificial Intelligence*, 14 (2), 167–181.
Zeleny, M., 1973. *In*: J.L. Cocchrance and M. Zeleny, eds. *Compromise Programming in Multiple Criteria Decision Making*. Columbia: University of South Carolina Press, 262–301.